Agricultural and Forest Meteorology 266–267 (2019) 129–139

Contents lists available at ScienceDirect

Agricultural and Forest Meteorology

journal homepage: www.elsevier.com/locate/agrformet

Spatial and temporal variations of N_2O emissions from global forest and grassland ecosystems

Kerou Zhang[a,d], Qiuan Zhu[a,*], Jinxun Liu[b], Meng Wang[a], Xiaolu Zhou[c], Mingxu Li[a], Kefeng Wang[a], Juhua Ding[a], Changhui Peng[a,c,*]

[a] Center for Ecological Forecasting and Global Change, College of Forestry, Northwest A&F University, Yangling 712100, China
[b] Western Geographic Science Center, US Geological Survey, Menlo Park, CA 94025, USA
[c] Institute of Environment Sciences, Department of Biology Sciences, University of Quebec at Montreal, Case Postale 8888, Succursale Centre-Ville, Montreal Quebec H3C 3P8, Canada
[d] Research Institute of Wetlands, Chinese Academy of Forestry, Beijing 100091, China

ARTICLE INFO

Keywords:
Nitrous oxide
Climate change
Process-based model
Global forest and grassland ecosystems

ABSTRACT

A process-based dynamic ecosystem model of TRIPLEX-GHG was used to estimate the spatial and temporal patterns of N_2O fluxes from global forest and grassland ecosystems under the effects of global warming and elevated CO_2 concentrations. From 1992 to 2015, the estimated average N_2O emissions from forests and grasslands were 3.62 ± 0.16 Tg N yr^{-1} and 1.40 ± 0.03 Tg N yr^{-1}, respectively. Tropical regions made large contributions (83.9% for forests and 74% for grasslands) to the total N_2O budgets, which were due to the larger N_2O flux values and large natural forest and grassland areas. The regional variations in N_2O emissions mainly resulted from the differences in the spatial distributions of climate characteristics, especially the precipitation patterns. In addition, anomalous years when N_2O emissions were relatively low/high were mainly due to the changes in climate patterns, which may have been induced by El Niño/La Niña events with different strengths and frequencies. Soil N_2O emissions from forests showed a positive effect on the atmospheric N_2O concentrations during June to November (R^2: 0.14˜0.28), while those from grasslands showed a positive effect during the growing seasons (R^2: 0.17˜0.28). Although natural N_2O sources (forests and grasslands in this study) showed slightly increasing trends, with 9.9 Gg N increment per year for forests and 2.1 Gg N increment per year for grasslands, they were not the main contributors to the elevated N_2O concentrations.

1. Introduction

Nitrous oxide (N_2O) is a principal greenhouse gas (GHG) that has a relative global warming potential that is 298 times that of CO_2 over a 100-yr period (IPCC, 2013). Moreover, N_2O contributes approximately 7% to radiative forcing (Artaxo et al., 2007), and it is also one of the largest ozone-depleting substances emitted from the biosphere (Ravishankara et al., 2009). Atmospheric N_2O has increased by 21% compared to the preindustrial level, and N_2O concentration reached 325.9 ppb per year in 2013 (Ciais et al., 2014). Natural N_2O emissions play important roles in determining the total emissions and feedback between the atmosphere and biosphere. N_2O emissions from natural forests and grasslands account for approximately 15–55% and 9–20% of the total N_2O emissions, respectively (Tian et al., 2013, 2016; Xu and Prentice, 2008; Zhuang et al., 2012). Furthermore, natural N_2O emissions are closely connected with climatic and ecological variables. The complex interactions among emissions, climate and ecological variables has contributed to the large uncertainty in the estimations of N_2O emissions from natural soils (Butterbach-Bahl et al., 2013; Chatskikh et al., 2005). Additionally, climatic and ecological variables also constitute potentially important feedbacks in the global earth system; for example, terrestrial N_2O emissions are enhanced under warmer climates and higher atmospheric CO_2 concentrations (van Groenigen et al., 2011; Xu et al., 2012). The associated feedback loop amplifies anthropogenic climate change and is reflected in paleontological records on glacial–interglacial and centennial timescales (Cai et al., 2014; Stocker et al., 2013). These potential roles of natural N_2O emissions in the climate system highlight the importance of the scientific understanding of the key processes that govern the production of emissions as well as accurate predictions of changes in emissions resulting from a changing climate.

Plenty of in situ N_2O experiments have been conducted throughout

* Corresponding authors at: Center for Ecological Forecasting and Global Change, College of Forestry, Northwest A&F University, Yangling 712100, China.
E-mail addresses: zhuqa@nwsuaf.edu.cn (Q. Zhu), peng.changhui@uqam.ca (C. Peng).

https://doi.org/10.1016/j.agrformet.2018.12.011
Received 14 June 2018; Received in revised form 19 December 2018; Accepted 20 December 2018
Available online 26 December 2018

the world over the past several decades (Williams et al., 1992; Abalos et al., 2016; Zhuang et al., 2012; Zhang et al., 2017); however, upscaling field observations from a site level to a regional or global scale is a great challenge. Several upscaling studies on N_2O emissions have been published using different approaches, such as the flux empirical extrapolation method (Zhuang et al., 2012), inverse method (Thompson et al., 2013) and process-based models (Zhang et al., 2017; Tian et al., 2018). Neither extrapolation nor inverse methods provide insight about the processes that are primarily responsible for GHG emissions or how to adequately characterize the full heterogeneity present in the landscape; therefore these methods involve large uncertainties when estimating regional emissions. In contrast, process-oriented models are often based on a better understanding of the biogeochemistry of GHG production and consumption (e.g., nitrification and denitrification); these models are considered powerful research tools for estimating regional and global N_2O emissions (Tian et al., 2018). Some global N_2O models attempt to simulate the global emissions of N_2O by considering a variety of complex regulating parameters or synthesizing the available flux measurements and known sources (Kiese et al., 2003, 2005; Li et al., 1992; Potter et al., 1996; Saikawa et al., 2013; Tian et al., 2013; Werner et al., 2007; Xu et al., 2012). However, there are still large uncertainties in terms of model calibration and validation, and large divergences exist when simulating the spatial and temporal variations of N_2O emissions with different models (Tian et al., 2013).

A better understanding of the N_2O emissions from natural forests and grasslands and how these emissions may change over time could help us better determine the impacts of N_2O and help policy-makers make better decisions when they are debating regulations for anthropogenic sources of N_2O. TRIPLEX-GHG model has already been calibrated and validated in simulating N_2O emissions across different ecosystems and latitudes in our previous study (Zhang et al., 2017). This study is the first application of this model for global N_2O estimation. The specific objectives of this study include 1) providing an updated estimate of N_2O budgets for global natural forests and grasslands using the TRIPLEX-GHG model, which may help narrow down the ranges of N_2O emission estimations from terrestrial ecosystems; 2) simulating temporal and spatial patterns of N_2O emissions under the impacts of multiple climate factors and analyzing the primary cause of N_2O emission anomalies; 3) exploring the relationships between soil N_2O emissions from natural forests and grasslands and the atmospheric N_2O concentrations.

2. Methodologies and model

2.1. Data description

In this study, we applied a series of spatiotemporal data sets to represent environmental changes at a spatial resolution of 0.5° × 0.5° latitude/longitude from 1992 to 2015. These data include daily climate conditions, such as the minimum, average and maximum temperature, precipitation, specific humidity, air pressure and wind speed. The climate data were downloaded from the CRUNCEP website (https://www.earthsystemgrid.org/dataset/ucar.cgd.ccsm4.CRUNCEP.v4.TPHWL6Hrly.html). The soil classification map used in this study included soil texture (clay, sand and silt fraction) and soil pH and was based on the Digital Soil Map of the World (DSMW), which we obtained from the FAO/UNESCO Soil Map of the World (http://www.fao.org/soils-portal/soil-survey/soil-maps-and-databases/faounesco-soil-map-of-the-world/en/) and conjoined the DSMW attributes with the soil properties dataset using methods in Batjes (2006). The soil C data and soil C:N ratio data were adopted from the global soil dataset (IGBP-DIS; 2000). The topographic input data were generated based on a global digital elevation model (DEM) with an approximate spatial resolution of 1 km (GTOPO30). The annual vegetation maps were aggregated from the annual maps from the Climate Change Initiative land cover project led by the European Space Agency (ESA − CCI − LC), which span cover a period of 24 years from 1992 to 2015 at a spatial resolution of 300 m (ESA, 2017, http://maps.elie.ucl.ac.be/CCI/viewer/). These maps describe the terrestrial surface of the Earth in 37 original land cover (LC) classes based on the United Nations Land Cover Classification System (UN-LCCS) (Di Gregorio, 2005). These data were developed by combining the global daily surface reflectance of 5 different observation systems, and the data accuracy was evaluated at a global scale (ESA, 2017). All datasets were transformed and re-projected to the same projection system and resolution (0.5° × 0.5°). The in situ data sampled from the atmosphere at the Mauna Loa Observatory (Keeling et al., 2005) in Hawaii was utilized as the atmospheric CO_2 concentration data used during the period of 1958-2015. The data before 1958 were mainly from the IS92a annual global CO_2 concentration dataset, and this dataset was obtained by spline fitting ice core data to the Mauna Loa sample data (Enting et al., 1994).

The global monthly means of atmospheric N_2O concentration used in this study were obtained from the combined Global Monitoring Division (GMD) N_2O data set (https://www.esrl.noaa.gov/gmd/hats/combined/N2O.html). The data set was developed by incorporating all of the monthly mean measurements of halocarbons and other atmospheric trace species (HATS) collected by several programs (e.g., old HATS flask instruments, current HATS flask instruments (OTTO), the Carbon Cycle Greenhouse Gases (CCGG) flask instruments (MAGIC), in situ HATS measurements (RITS program and CATS programs)), and they were calculated by taking the weighted averages of co-located measurements from background NOAA/ESRL GMD air measurement programs.

2.2. Model description

TRIPLEX-GHG is a process-based model that is primarily based on the integrated biosphere simulator (IBIS) (Foley et al., 1996) and the denitrification decomposition (DNDC) model (Li et al., 2000). The TRIPLEX-GHG model consists of six basic submodules: a land surface submodule, a vegetation dynamic submodule, a plant phenology submodule, a soil biogeochemical submodule, a methane (CH_4) submodule (Zhu et al., 2014, 2015) and a N_2O submodule (Zhang et al., 2017). These submodels are coupled to estimate the fluxes and pool size of carbon, nitrogen, water and three main greenhouse gases (CO_2, CH_4, N_2O) in terrestrial ecosystems at spatial scales ranging from site to regional and global scales, and time steps from hourly to yearly. The first five submodules mainly create the atmosphere-vegetation-soil system through representing energy-water exchange processes, vegetation dynamics, canopy physiology, and C and N flows for each plant functional types (PFTs) (Foley et al., 1996; Kucharik et al., 2000; Liu et al., 2005; Zhu et al., 2014). For each PFT, model balances carbon between surface and belowground carbon litter pools derived from litterfall, and soil organic matter pools of differing decomposability following Parton et al. (1987) and Verberne et al. (1990). The dynamics of the soil N pool are calculated based on the C:N ratio specified by PFT (Kucharik et al., 2000). Soil mineral N is considered to be the primary indicator of N availability. It was regulated by the decomposition of belowground litter pools, the plant uptake determined from N demand and N storage, ammonia volatilization, leaching and microbial dynamics (Foley et al., 1996; Kucharik et al., 2000). It also has feedbacks by limiting both the ecosystem C flux and the C:N ratios of the different fluxes associated with growth respiration and decomposition (Liu et al., 2005). Detailed information that describe the first five submodules could be found in the supplemental material and the key equations related to carbon balance are shown in Table S1. In the N_2O submodule, the major biochemical processes that regulate N_2O formation include nitrification and denitrification (Zhang et al., 2017). The decomposition process forms the linkage between N_2O production and consumption pathways and soil C and N cycles in the biogeochemistry submodule. Organic C is either oxidized to CO_2 through microbial respiration or transferred to soluble carbon or other carbon substrates. Organic N is mineralized to

ammonium (NH_4^+), which is then nitrified to nitrate (NO_3^-), and these nutrients are important nutrients for nitrifiers and denitrifiers. In our model, part of the N_2O is produced through the process of biological oxidation of NH_4^+ to NO_2^- and NO_3^- (nitrification pathway). The residual N_2O was produced from denitrification, which is designed to be a "chain reaction" process: the reduction of nitrate to forms nitrous oxide and molecular nitrogen. Production of N_2O by denitrification occurs when bacteria that are capable of denitrification colonize a location where oxygen is essentially absent and water, nitrate and decomposed organic compounds are present. When modeling these two microbe-based processes, the microbial activities of nitrifying and denitrifying bacteria are explicitly included based on the Michaelis–Menten equations (Michaelis and Menten, 1913), and the "anaerobic balloon" concept (Li et al., 2000) is used to regulate the rates of the allocation of substrates (e.g., DOC, NH_4^+, and NO_3^-) to both processes. More detailed information can be found in Zhang et al. (2017).

2.3. Model validation and simulations

The model has been calibrated at a global scale using daily data, and was found to perform reasonably well based on validation results in our previous study (totally 81 sites from natural forests and grasslands where little or no anthropogenic disturbances have taken place) (Zhang et al., 2017). Specifically, considering that the nitrification and denitrification processes were first coupled into the model, it is necessary to calibrate the key model parameters related to nitrification and denitrification to increase model reliability to simulate N_2O fluxes. Therefore, prior to calibration, the most sensitive parameter which strongly affect the N_2O fluxes outputs was identified for site-specific studies. Sensitivity analysis for selected 23 parameters was carried out and the maximum nitrification rate coefficient (COE_{NR}) was found to be the most sensitive one. The optimized value of this parameter was obtained using parameter fitting for 29 calibration sites. Based on biome-type forest regions (tropical forests, temperate forests and boreal forests) and grasslands, an average parameter value for all data collection sites in that region was calculated (Table 1). To support the result of model validation, the simulation of the primary factors (soil temperature and water-filled porespace (WFPS)) was also tested by comparing the measurements for some sites where data are available. The seasonal variations and magnitudes of simulations were good overall, and annual observation and simulation data were highly correlated ($R^2 = 0.75$). In this study, simulations were conducted with the parameter at the global level.

To qualify the effect of climate variability and land cover transition on N_2O fluxes, the potential effects of atmospheric deposition and land management practices were excluded from the model simulations. The model simulation went through an initial 300-year spin-up procedure. The initial 300-year spin-up was driven with multi-year (between 1901 and 1920) averaged historical meteorological data to achieve a relative equilibrium state in the carbon pools before analysis. For reaching soil carbon equilibrium, the model has an internal speed-up process during the soil spin-up period. After spin-up, the model was run starting from 1901 using daily climatological data from CRUNECP and atmospheric CO_2 data based on ice core and atmospheric measurements for transient simulations (Keeling et al., 2005). The global vegetation map used for model initial simulation from 1901 to 1991 was generated from the GlobCover 2009 land cover map (original spatial resolution: 300 m) (Bontemps et al., 2010), and the ESA − CCI − LC (annual land cover map available during the period of 1992–2015) was used for subsequent simulations. Only result of 1992–2015 were extracted for analysis.

Table 1
Parameter (the maximum nitrification coefficient, COE_{NR}) based on the biome type of observation sites for global forests and grasslands N_2O emissions modeling.

Biome	COE_{NR}	SEM	Site numbers	Data records
Boreal forests	0.09	0.0136	4	126
Temperate forests	0.04	0.0124	15	665
Tropical forests	0.009	0.0018	4	200
Grasslands	0.03	0.0047	6	333

SEM: standard error of the mean.

2.4. Trend and correlation analysis

The total N_2O emission (T) and the area-weighted average N_2O flux (F_s) are calculated as follows:

$$T = \sum_{j=1}^{n} F_j \bullet S_j$$

$$F_s = \frac{T}{\sum_{j=1}^{n} S_j}$$

where n is the total number of grids of forests or grasslands; F*j* and S*j* are the N_2O flux and the area of the jth grid, respectively. The vegetation type for an individual grid in each year is classified based on the annual ESA − CCI − LC maps.

The trends of N_2O emissions for individual grid cells were identified using the Mann-Kendall test. The Mann-Kendall test is a nonparametric technique (Mann, 1945; Kendall, 1948) that is widely used in hydrology and climatology. The Mann-Kendall statistic indicates the direction and magnitude of the trend in simulated natural N_2O emissions. In the Mann-Kendall trend test for a set of elements, n is the total number of elements; here we used the total number of annual data. The Mann-Kendall rank test statistic S is given by:

$$S = \sum_{k=1}^{n-1} \sum_{j=K+1}^{n} Sgn(X_j - X_k)$$

$$Sgn(X_j - X_k) = \begin{cases} 1 & (X_j - X_k) > 0 \\ 0 & (X_j - X_k) = 0 \\ -1 & (X_j - X_k) < 0 \end{cases}$$

where n is the total number of elements; X_j and X_k are the jth and kth elements ($j \le n$, and $k \ne j$).

In the absence of any trend (H_0 or null hypothesis), the function of S can be assumed to have a normal distribution, with the expected variance var(S) given by:

$$var(S) = \sigma^2 = n \bullet (n-1) \bullet (2n+5)/18$$

The standard normal distribution Z is given by:

$$Z = \begin{cases} (S-1)/\sqrt[2]{var(S)} & S > 0 \\ 0 & S = 0 \\ (S+1)/\sqrt[2]{var(S)} & S < 0 \end{cases}$$

The distribution of the test statistic Z is compared with a standard normal distribution at a certain level of significance, and the significance level is set to be 0.05 in this study. Therefore, the no trend or H_0 hypothesis is rejected for high values of $|Z| \ge 1.96$, and the trend is considered increasing when Z is greater than 0. We mapped the spatial pattern of this statistic for modeled N_2O emissions to identify significant trends. Furthermore, Spearman correlation analysis was used to estimate the correlation between the N_2O fluxes and the model-driven data over the time series (i.e., the input climate data). All statistical analyses were performed using the open-source software R version 3.2.0 (R Foundation for Statistical Computing, Vienna, Austria).

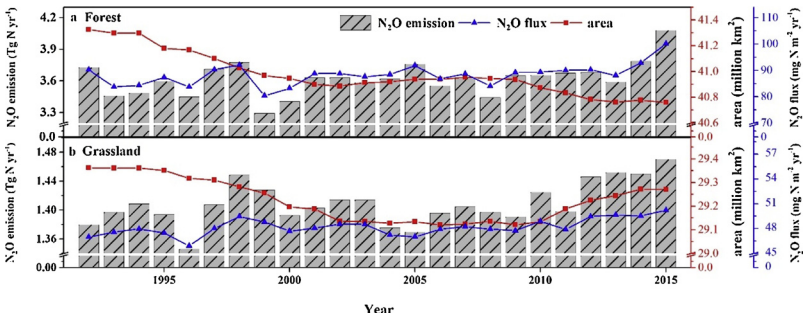

Fig. 1. Interannual variations of N_2O emissions, N_2O fluxes and areas of global forests (a) and grasslands (b). The N_2O emission means the total emission calculated by summing the products of N_2O flux and area; the N_2O flux means the per unit area N_2O emission.

3. Results

3.1. Forest and grassland N_2O emission budgets at global, biome and continental scales

As shown in Fig. 1, the estimated total global forest areas decreased from 41.76 million km^2 to 41.32 million km^2. The global area-weighted mean N_2O flux from forests from 1992 to 2015 was 88.3 ± 4.0 mg N m^{-2} yr^{-1}, ranging from 80.3 mg N m^{-2} yr^{-1} (1999) to 100.1 mg N m^{-2} yr^{-1} (2015). The estimated average total N_2O emissions from forests from 1992 to 2015 was 3.62 ± 0.16 Tg N yr^{-1}, ranging from 3.29 Tg N yr^{-1} (1999) to 4.08 Tg N yr^{-1} (2015).

The estimated total global grassland areas first decreased until 2004 and then increased from 2004 to 2015, with the average increase of 29.2 ± 0.09 million km^2 yr^{-1}. The global area-weighted mean N_2O flux from grasslands from 1992 to 2015 was 48.2 ± 1.0 mg N m^{-2} yr^{-1}, ranging from 45.9 mg N m^{-2} yr^{-1} (1996) to 50.2 mg N m^{-2} yr^{-1} (2015). The estimated total N_2O emissions from grasslands from 1992 to 2015 was approximately 1.40 ± 0.03 Tg N yr^{-1}, ranging from 1.35 Tg N yr^{-1} (1996) to 1.47 Tg N yr^{-1} (2015). Moreover, N_2O emissions showed slightly increasing trends for both forests (mean increase of 9.9 Gg N yr^{-1}) and grasslands (mean increase of 2.1 Gg N yr^{-1}) over the study period. Approximately 83.9% and 74% of the total emissions were from forests and grasslands in tropical regions, respectively. Boreal regions contributed a smaller proportion of N_2O emissions than contributed by areas in tropical regions or other biomes (Table 2, Figs. S1, S2). The modeled total budget of annual N_2O emissions from global forests and grasslands can be found in Table S2.

At the continental scale, South America showed the highest N_2O emissions from both forest and grassland ecosystems, which is caused by the large N_2O fluxes compared to other continents (Table 3). Africa and South America acted as the largest forest and grassland N_2O sources as they had the highest N_2O fluxes and the largest natural forest and grassland areas, suggesting that Africa and South America play major roles in the global N_2O budget at the continental scale.

3.2. Spatial distribution and trends of N_2O fluxes

Fig. 2a, b shows the spatial distribution of N_2O fluxes in forests and grasslands, respectively. Rate of N_2O released greater than 550 mg N m^{-2} yr^{-1} were found in tropical and subtropical forest regions and savannas due to the greater availability of substrate and favorable climate conditions for nitrifiers and denitrifiers. However, the large boreal forest areas in northern high-latitude regions were less-substantial N_2O emission sources (< 20 mg N m^{-2} yr^{-1}). Fig. 2c, d shows the results of the Mann-Kendall trend test for N_2O fluxes in forests and grasslands. Most regions showed increasing simulated N_2O fluxes, and significant increases were found in tropical forests, such as the Amazon plain and Central Africa, subtropical forests in southeastern China and southwest Europe and boreal forests in Eastern and Central Russia. Some areas (grid cells) that were mainly distributed along the Eastern Andes and Southeast Asia showed significant decreasing trends. Grasslands located in northern North America, Pampas in Africa, Inner Mongolia in China and southwest Australia showed significant decreases in simulated N_2O fluxes, while the majority of grid cells in Africa showed significant increasing trends.

3.3. Seasonal trends in N_2O fluxes and emissions in global forests and grasslands

Fig. 3 shows the seasonal variations of N_2O fluxes along a zonal gradient and total N_2O emissions. There are distinct seasonal cycles in the N_2O emissions from natural forests and grasslands. Forests emissions from Northern Hemisphere and Southern Hemisphere both exhibited one seasonal peak, with the peak emissions occurring in July (0.284 ± 0.016 Tg N m^{-2} $month^{-1}$) and December (0.197 ± 0.013 Tg N m^{-2} $month^{-1}$), respectively. It is obvious that the seasonal variations amplitudes in simulated global forest N_2O emissions from Northern Hemisphere were larger than that from Southern Hemisphere. For grasslands, the seasonal variation of emissions showed an opposite trend. For example, the highest emission occurred in July (0.107 ± 0.005 Tg N m^{-2} $month^{-1}$) and lowest in December (0.837 ± 0.004 Tg N m^{-2} $month^{-1}$) from Northern Hemisphere, and the highest emission occurred in January (0.085 ± 0.005 Tg N m^{-2} $month^{-1}$) and lowest in June (0.326 ± 0.002 Tg N m^{-2} $month^{-1}$) from Southern Hemisphere. The increases in solar radiation and growing season length from north to south could be responsible for the existing pattern. Although, Northern Hemisphere N_2O emissions from both grasslands and forests were higher than that in Southern Hemisphere, it is based on a fact that the Northern land area is larger than the south. For forests and grasslands, the average N_2O fluxes along the altitudinal gradient first spread

Table 2
Average percentages of total N_2O emissions and total areas of forests and grasslands in different biomes from 1992 to 2015 (the values are denoted as mean ± SD (standard deviation)).

Percentage of total amount	Ecosystem type	Boreal region	North temperate region	Tropical region	South temperate region
N_2O emissions	Forest	1% ± 0.15%	13.8% ± 1%	83.9% ± 1%	1.3% ± 0.08%
	Grassland	0.9% ± 0.15%	18% ± 0.7%	74% ± 0.7%	7.1% ± 0.3%
Total area	Forest	15.6% ± 0.09%	33.3% ± 0.17%	49.4% ± 0.26%	1.7% ± 0.01%
	Grassland	8.4% ± 0.15%	34.5% ± 0.14%	50.1% ± 0.26%	7% ± 0.03%

Table 3
Average N_2O fluxes, areas and emissions from forests and grasslands on different continents from 1992 to 2015 as simulated by the TRIPLEX-GHG model (the values are denoted as mean ± SD (standard deviation)).

	Forest			Grassland		
Continents	N_2O emission (Tg N yr^{-1})	Area (million km^2)	N_2O flux (mg N m^{-2} yr^{-1})	N_2O emission (Tg N yr^{-1})	Area (million km^2)	N_2O flux (mg N m^{-2} yr^{-1})
Asia	0.71 ± 0.037	12.7 ± 0.05	60.0 ± 3.0	0.22 ± 0.01	8.1 ± 0.04	26.9 ± 1.4
North America	0.36 ± 0.02	7.7 ± 0.03	46.8 ± 2.5	0.20 ± 0.007	5.33 ± 0.015	37.6 ± 1.23
Europe	0.053 ± 0.006	3.5 ± 0.012	15.13 ± 1.63	0.025 ± 0.002	1.18 ± 0.02	20.6 ± 1.6
Africa	1.18 ± 0.036	7.03 ± 0.04	167.6 ± 4.46	0.40 ± 0.008	7.0 ± 0.13	57.6 ± 1.5
South America	1.26 ± 0.11	7.88 ± 0.16	160.3 ± 13.9	0.45 ± 0.016	4.42 ± 0.04	102.55 ± 3.2
Oceania	0.054 ± 0.004	0.72 ± 0.0023	74.8 ± 5.2	0.11 ± 0.009	3.18 ± 0.02	34.8 ± 2.7

southwards and then northwards throughout the year. The relatively high level of monthly N_2O fluxes from forests (generally more than 20 mg N m^{-2} $month^{-1}$) occurred between 30 °N and 40 °N during summer, while in grasslands, they occurred near 20 °N in Spring.

3.4. The correlation between climate forcings and global N_2O fluxes from global forests and grasslands

Fig. 4 shows the Spearman correlations between global N_2O fluxes and precipitation (Fig. 4a, b) and temperature (Fig. 4c, d). Compared with air temperature, precipitation is the dominant controller that regulates the N_2O fluxes from the majority of forests and grasslands. For global forests and grasslands, the total number of grids where the N_2O flux is significant correlated to the precipitation and temperature are 16,385 and 6369, which accounted for approximately 55.3 and 21.5 percent of total grids, respectively. And about 25.3 percent of grids showed the correlation coefficient between N_2O flux and precipitation was bigger than 0.5 with significance. In most boreal forest ecosystems, N_2O fluxes were positively correlated with precipitation and specific humidity, while they were not significantly correlated ($P > 0.05$) with other climate variables (Figure S3). For tropical forest regions, N_2O fluxes were significantly negatively correlated with precipitation in the majority of tropical forest regions areas, except for some scattered regions in the Congo Basin that showed positive correlations.

In the majority of grassland ecosystems, precipitation was positively correlated with N_2O fluxes. Precipitation was positively correlated with the N_2O fluxes in most of the temperate grassland regions in the Southern Hemisphere, except for those in Madagascar, Africa. Furthermore, temperature and precipitation showed opposite effects on the N_2O fluxes from grasslands in Australia, while they showed consistent effects in Eastern Russia and the Qinghai-Tibet Plateau in China.

3.5. The relationship between N_2O emissions and El Niño–southern oscillation (ENSO)

Fig. 5 shows the spatial distributions of N_2O fluxes, precipitation and temperature increases (the value in 1998 minus that in 1999) for tropical forests. The N_2O flux in most tropical forests appeared to decrease at various degrees. Specifically, between 1998 and 1999, there were reductions of more than 300 mg N m^{-2} yr^{-1} in the N_2O fluxes in the Orinoco plain and northeast Amazon Plain in South America. To illustrate the relationship between tropical N_2O emissions and the ENSO, the monthly mean anomaly fluxes of N_2O in tropical forests and grassland ecosystems during the experimental periods were performed according to La Niña and El Niño events. According to Fig. 6, the monthly mean anomaly fluxes of N_2O tend to be greater than zero during strong and very strong La Niña events periods for tropical forests, which indicates an increase of N_2O emissions comparing the average level. The monthly mean anomaly fluxes of N_2O tend to be less than zero during strong and very strong El Niño events, which indicates a decrease of N_2O emissions. For grassland ecosystem, the monthly mean anomaly fluxes of N_2O during La Niña and El Niño events varies without regularity. Fig. 7 shows the differences in the area-weighted mean monthly N_2O fluxes from tropical forests and grasslands between La Niña or El Niño months and neutral months. The responses of N_2O release from tropical forests to El Niño events exhibit the opposite pattern (Fig. 7a). The N_2O fluxes during El Niño months are larger than those during neutral months. For grasslands in the tropics, wet months (generally from May to October) during El Niño/La Niña years showed relatively higher/lower average N_2O fluxes, while dry months (generally from November to the following April) during El Niño/La Niña years showed relatively lower/higher average N_2O fluxes than those in the corresponding months in neutral years (Fig. 7b).

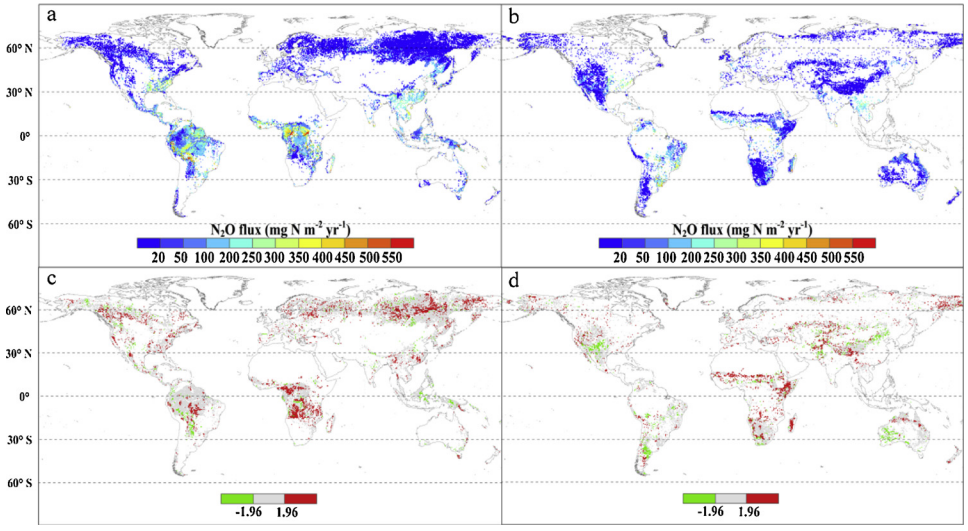

Fig. 2. Spatial patterns of the average N_2O fluxes for forests (a) and grasslands (b); Mann-Kendall statistics in forests (c) and grasslands (d) simulated for 1992–2015.

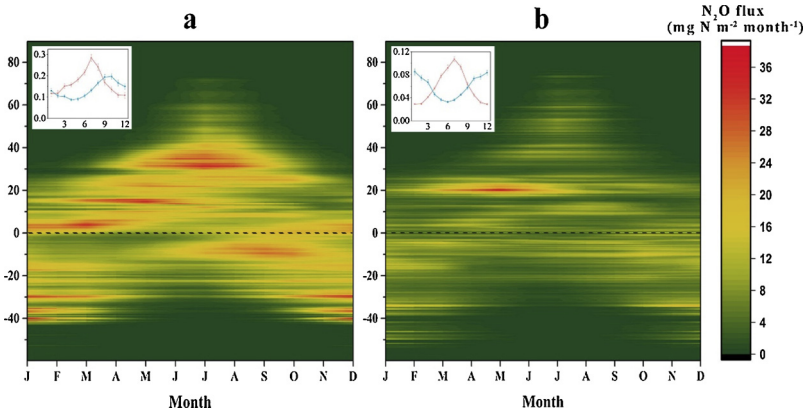

Fig. 3. Variations of area-weighted average N_2O fluxes and total emissions (Tg N month^{-1}, graphs at the left upper corner) from forests (a) and grasslands (b) along with the latitudinal gradient (by 1°) at a monthly step. For the graphs at the left upper corner, the red line represents N_2O emissions from the Northern Hemisphere, and the blue line represents N_2O emissions from the Southern Hemisphere (For interpretation of the references to colour in this figure legend, the reader is referred to the web version of this article).

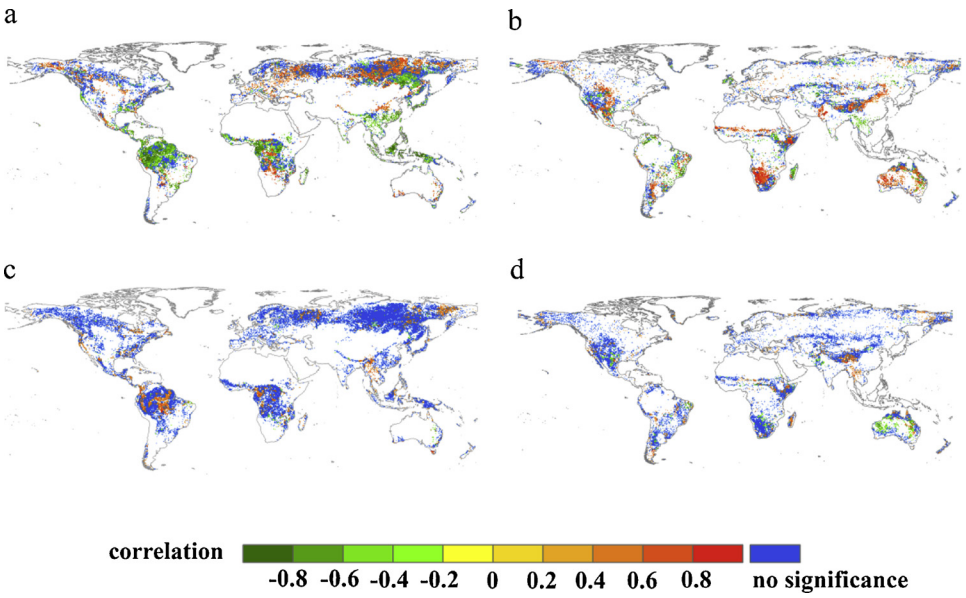

Fig. 4. Correlations between N_2O fluxes and precipitation in forests (a) and grasslands (b), and between N_2O fluxes and temperature in forests (c) and grasslands (d). Non-significant correlations are shown in blue (For interpretation of the references to colour in this figure legend, the reader is referred to the web version of this article).

3.6. The relationship between soil N_2O emissions from forest and grasslands and atmospheric N_2O concentrations

Overall, the correlation between soil N_2O emissions and atmospheric N_2O concentrations was low (Figure S4, $R^2 = 0.26$) when the sum of the emissions from forests and grasslands was considered which implies that approximately 25.9% of total observed annual N_2O increases in the atmosphere can be explained by these natural emissions (forests and grasslands). The significant correlations were mainly attributed to strong N_2O concentration variations for specific months. From June to November, soil N_2O emissions from forests are significantly positively correlated with the atmospheric N_2O concentrations, as the N_2O emissions from forests are larger from June to November than those in other months (Figs. 3a, 5). For grassland ecosystems, soil N_2O emissions have significant positive correlation to the atmospheric N_2O concentrations in January, September, October and November (Table 4), however, it may be caused by the co-correlated with positive relationship between concentration and emissions in forest, based on the fact the overall grassland emissions are much smaller than forest emissions.

3.7. Sensitivity analysis of spatial estimation

Sensitivity experiments have been conducted for different climate variables, including the precipitation and air temperature. The value of a single input parameter is changed (± 25% for precipitation and ± 0.5°C for air temperature) relative to its original value, with other parameters held fixed. In addition, we applied the simplified Most Significant Factor (MSF) method to estimate the uncertainties induced by parameters that are fluctuated in a certain range (Li et al., 1996; Giltrap et al., 2010). The MSF method involves taking the extreme values of the factor(s) producing most of the variation in the model predictions and can be used in most regional simulations with low computationally expensive. The key parameter COE_{NR} was only conducted the MSF method, since it turns out from our model study (Zhang et al., 2017) to be the most sensitive parameter in controlling N_2O emissions to the atmosphere and it differs in biome regions when conducting the regional simulation.

The N_2O emission amounts resulting from each run are then compared with the result from the standard run (SS) for different biome regions (Table 5). For tropical and temperate forests, the climate variables have a significant effect on global N_2O emissions. The total emissions have been changed more than 10% for changing 25% of precipitation and changing 0.5°C of air temperature. However climate variables seem to have relatively weak influence on N_2O emissions from boreal regions. The precipitation variation has opposite effect on tropical forests N_2O emissions compared to air temperature, for example, the emissions increasing by 0.53 Tg N yr^{-1} when the precipitation is decreased by 25%. Air temperature performed positive effect on all regions of global forests and grasslands, with about 26% increase and 53% decrease in total N_2O emissions when the air temperature is increase and decrease 0.5°C, respectively. Based on the MS and NS

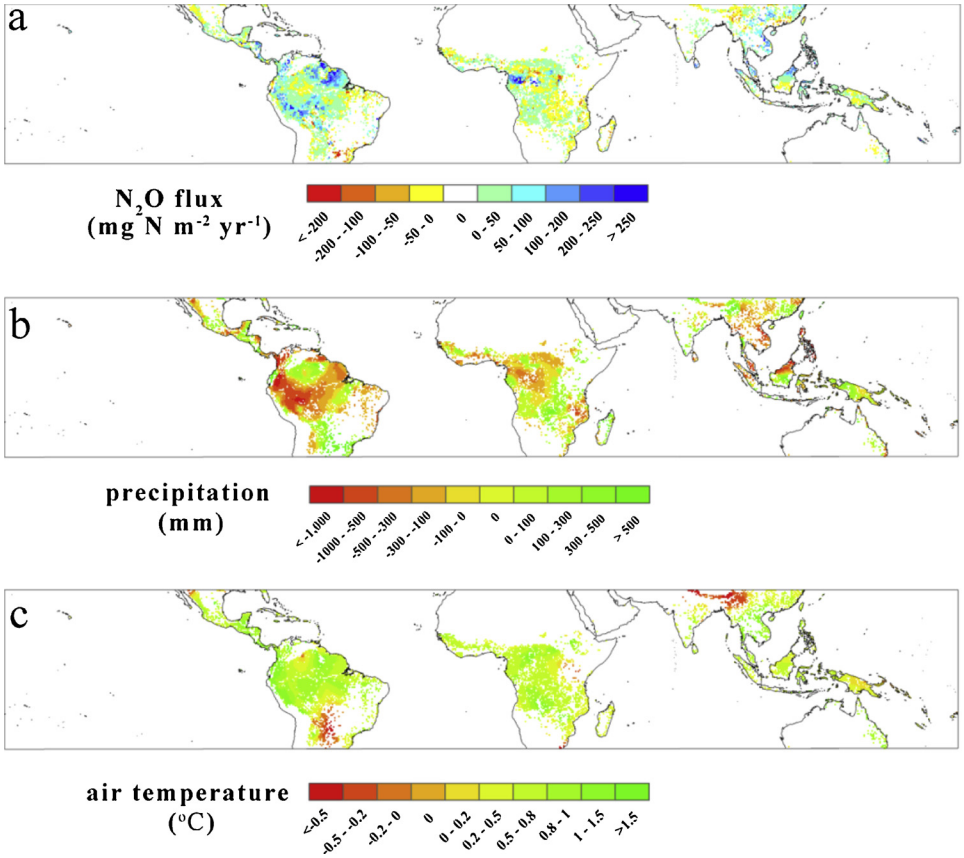

Fig. 5. Spatial distributions of N_2O fluxes, precipitation and temperature increases (the value in 1998 minus that in 1999) for tropical forests.

scenarios (Table 5), the extreme COE_{NR} values for every biome regions produced a range of N_2O emission predictions (about -14.6%~+11.9%). Furthermore, the variation of COE_{NR} may not change the trends of N_2O emissions during the period of 1992–2015.

4. Discussion

4.1. Comparisons with previous studies

The total predicted N_2O emissions of 3.62 Tg N per year from forests and 1.41 Tg N per year from grasslands during the study period are both within the range of previously reported values. Tian et al. (2013) reported average N_2O emissions of 4.28 Tg N per year from global forests and 3.64 Tg N per year from global grasslands over 1981-2010. The lower N_2O estimates of our study may be due to the effects of additional global change factors such as tropospheric O_3, nitrogen deposition and nitrogen fertilizer use, which are not included in the model in this study, and these factors were reported to increase N_2O emissions via their influence on soil C and N balance (Gomez-Casanovas et al., 2016; Kanerva et al., 2008; Shcherbak et al., 2014; Xu et al., 2008). Moreover, Xu et al. (2008) also reported global N_2O emission rates of 6.99 Tg N per year for forests and 4.49 Tg N per year for grasslands from 2000 to 2008 by combining an empirical climate-driven soil respiration model (Raich et al., 2002) (driven by air temperature and precipitation) with the linear functions of N_2O and CO_2 fluxes, which are obtained from a meta-analysis. The N_2O emissions estimated by Xu et al. (2008) are much higher than those estimated in this study, which may be due to overestimating of soil respiration and ignoring the effects of other important factors (e.g., soil pH) on N_2O emissions (Xu et al., 2008). Zhuang et al. (2012) reported values of 1.3 Tg N per year from forests and 1.31 Tg N per year from grasslands in 2000, and these values were extrapolated from field measurements by using an artificial neural network approach; the differences in the N_2O emissions from forests between the two studies may be caused by the differences in LC area estimates. In our study, the forest area was estimated to be 40.95 million km^2 (ESA–CCI–LC), and this estimated value is similar to the value estimated by Keenan et al. (2015) (40.55 million km^2 in 2000), while the forest area estimated by Zhuang et al. (2012) (Land Cover Type Yearly L3 Global CMG, MCD12C1; 26.03 million km^2 in 2000) is much smaller than that estimated in this study. The N_2O emissions from tropical forests were estimated to be within the range of 1.17–3.55 Tg N yr^{-1} (Breuer et al., 2000; Matson and Vitousek, 1990; Potter et al., 1996; Stehfest and Bouwman, 2006; Werner et al., 2007) during the 1990s, and the N_2O emissions from tropical forests estimated by our model (2.98 Tg N yr^{-1}) were within this range.

In addition, the global spatial patterns of N_2O fluxes obtained in this study are also consistent with the results of other studies (Saikawa et al., 2013; Xu et al., 2012; Zhuang et al., 2012). In general, boreal regions showed relatively low N_2O emissions (< 40 mg N m^{-2} yr^{-1}), while tropical regions (especially in rainforest area) showed relatively higher emissions (usually more than 200 mg N m^{-2} yr^{-1}). However, great uncertainty still exists in the estimation of N_2O fluxes in tropical regions (Tian et al., 2016). The N_2O fluxes estimated by this study in tropical regions showed significant spatial heterogeneity, and the estimations of N_2O fluxes in rainforest regions that were close to the equator could reach 685 mg N m^{-2} yr^{-1}; however, some areas showed extremely low N_2O fluxes (near zero). Conversely, in the study by Xu et al. (2012), the differences in N_2O fluxes from tropical regions were small; that is, the majority of places showed high N_2O emission levels. The results of Saikawa et al. (2013) showed that the N_2O emissions from southern Asia and Southeast Asia play major roles in the global N_2O budget, while in this study, the forests in Africa and South America that were close to the equator were the main sources of N_2O emissions. This finding indicates that tropical regions have become the areas with

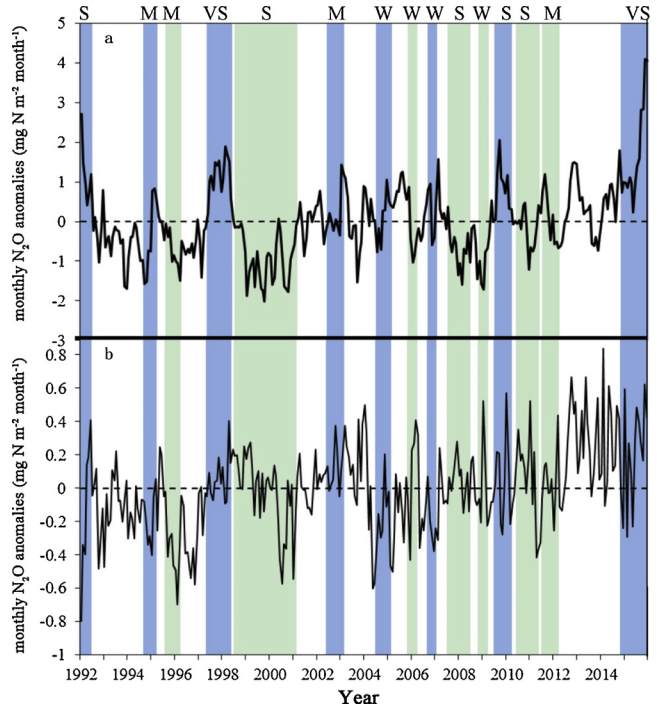

Fig. 6. Monthly mean anomaly fluxes of N_2O (total monthly emissions/total area) in tropical forest (a) and savanna (b) ecosystems between 1992 and 2015 (mg N m^{-2} $month^{-1}$). The green and blue areas represent the periods of La Niña and El Niño events respectively (S: strong; M: moderate; VS: very strong; W: weak, http://origin.cpc.ncep.noaa.gov/products/analysis_monitoring/ensostuff/ONI_v5.php) (Huang et al., 2017) (For interpretation of the references to colour in this figure legend, the reader is referred to the web version of this article).

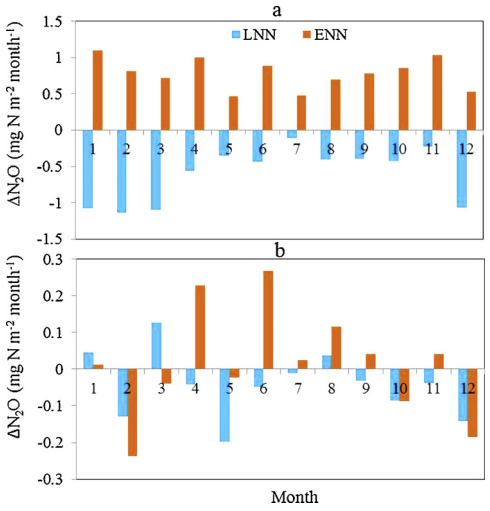

Fig. 7. Differences in the area-weighted mean monthly N_2O fluxes from tropical forests (a) and grasslands (b) between La Niña or El Niño months and neutral months. LNN and ENN represent the values derived from the area-weighted monthly mean N_2O fluxes from La Niña and El Niño months minus the area-weighted monthly mean N_2O fluxes from neutral months, respectively. The periods of La Niña and El Niño event are baseds on http://origin.cpc.ncep.noaa.gov/products/analysis_monitoring/ensostuff/ONI_v5.php.The mean and standard deviations of area-weighted monthly N_2O fluxes from forests and grasslands in neutral month, El Niño month and La Niña month can be found in Table S3.

high uncertainties in N_2O flux estimates. On the one hand, this fact is probably due to the effects of the different responses of climate factors (particularly under high rainfall and high temperature conditions) on N_2O emissions in different models. On the other hand, tropical regions have unique water thermal environment conditions and the geographical positions that result in the frequent occurrence of extreme climate events, which may be the cause of the large spatial heterogeneity of the N_2O emissions from tropical regions.

4.2. The relationship between N_2O emissions and El Niño–southern oscillation (ENSO)

The anomalous climate patterns in tropical regions were mainly induced by La Niña/El Niño events, and such anomalies from normal surface temperatures caused by La Niña/El Niño events can have large-scale impacts not only on ocean processes but also on global weather and climate. The mature La Niña from November 1998 to early 2001 was reported by Schwing et al. (2002), and this study revealed that the N_2O fluxes in the tropics decreased during this period. Similarly, the decreases in the total emissions in 1996 and 2008 were also preceded by sharp decreases in the N_2O fluxes in tropical regions that were coincident with anomalous climate patterns that were induced by the recorded La Niña events during the corresponding periods (Schwing et al., 2002). For example, the N_2O flux between 1998 and 1999 has large reductions, especially in the Orinoco plain and northeast Amazon Plain in South America, it can be ascribed to the substantial increase in precipitation induced by the La Niña events and as a result of the significant negative correlation between the N_2O flux and precipitation in tropical regions. Tropical forests N_2O flux during neutral months are less than those during El Niño months and larger than those during La Niña months. However, this is in contrast to the prevailing view that El Niño/La Niña events induce N_2O decreases/increases (Huang and Gerber, 2015; Saikawa et al., 2013; Thompson et al., 2013), it may be due to the different model performance under the high level of precipitation. In this study, excessive precipitation induced the decrease of N_2O fluxes for tropical regions. In addition, for grasslands in the tropics, N_2O fluxes during El Niño/La Niña events showed relatively higher/lower in wet months (generally from May to October) and lower/higher in dry months (generally from November to the following April) comparing the neutral months. This response may be attributed to the tropical savanna climate, which has distinct dry and wet seasons. Greenhouse gasses (i.e., CO_2, N_2O and CH_4) have been proven to be sensitive to extreme climate events (Zhu et al., 2017; Gurney et al., 2012; Schwalm et al., 2011); thus, extreme climate events may become comprehensive and effective indicators that reflect the relationship between climate change and global greenhouse gas emissions.

4.3. The relationship between N_2O emissions from forests and grasslands and the atmospheric N_2O concentration

The interannual variations of N_2O emitted from natural forest and grassland soils showed slight correlations with the consistent increase in the atmospheric N_2O concentration, which implies that the increasing atmospheric N_2O concentration is mainly due to the elevation of other emission sources, such as emissions from anthropogenic, riverine and oceanic N_2O (Flückiger et al., 1999; Hu et al., 2016). Complicated processes, including gas diffusion and chemical reactions in the atmosphere (Ravishankara et al., 2009), are another reason for the low correlations between the atmospheric N_2O concentration and N_2O emissions from forests and grasslands. In addition, there is no distinct seasonal variation in the atmospheric N_2O concentration; however, we found that their correlations differed in different months. For example, soil N_2O emissions from forests during summer and autumn have positive effects on the atmospheric N_2O concentrations, while no significant correlations were found in spring and winter. This result might be related to the rapid growth rates of N_2O during summer and autumn

Table 4
The monthly mean atmospheric N_2O concentration and N_2O emissions from forests or grasslands and their correlations.

	Atmospheric N_2O concentration (ppm)		N_2O emissions from forests (Tg N month^{-1})			N_2O emissions from grasslands (Tg N month^{-1})		
Month	Mean	SD	Mean	SD	R^2	Mean	SD	R^2
1	317.991	5.617	0.246	0.022	0.006	0.114	0.005	0.274[a]
2	318.040	5.595	0.224	0.020	0.001	0.104	0.004	0.063
3	318.023	5.594	0.254	0.015	0.003	0.108	0.004	0.133
4	318.003	5.623	0.246	0.012	0.011	0.102	0.004	0.005
5	317.994	5.640	0.273	0.012	0.110	0.114	0.004	0.002
6	318.014	5.644	0.322	0.014	0.281[a]	0.124	0.006	0.060
7	318.068	5.648	0.416	0.018	0.143[a]	0.143	0.005	0.000
8	318.147	5.666	0.408	0.021	0.187[a]	0.139	0.004	0.008
9	318.251	5.693	0.363	0.024	0.256[a]	0.121	0.004	0.166[a]
10	318.404	5.728	0.333	0.022	0.257[a]	0.118	0.004	0.217[a]
11	318.545	5.756	0.276	0.023	0.155[a]	0.109	0.005	0.279[a]
12	318.683	5.749	0.258	0.024	0.116[a]	0.112	0.004	0.039

SD: standard deviation.
[a] significant correlation.

and the relatively low or negative growth rates during spring and winter. Atmospheric N_2O concentrations significantly increased with the increase in soil emissions from grasslands in autumn, which is the growing season for grasses in the Southern Hemisphere. Thus, natural sources (forest and grassland ecosystems) are not the key contributors to the rising atmospheric N_2O concentration.

4.4. The relationship between N_2O emissions and the climate factors

Additionally, the model results show that the spatial and seasonal distributions of N_2O emissions are highly related to climate patterns (mainly the precipitation and temperature patterns). For most grasslands, increases in precipitation would favor the production of N_2O. Previous studies indicated that N_2O fluxes are sensitive to precipitation (Butterbach-Bahl et al., 2000; Li et al., 2000; Lu et al., 2008), since precipitation plays a dominant role in controlling soil moisture, which is vital to gas diffusion, denitrification and N_2O emissions. Increases in soil moisture provide anaerobic conditions for N_2O production and promote the decomposition of residual organic matter, enhancing the supply of nitrogen and carbon substrates for denitrification (Chen et al., 2013). In the tropics where temperature is not a limiting factor, moisture is the dominant factor for N_2O emissions. However, elevated precipitation was found to be negatively correlated with N_2O fluxes from tropical regions in our study, and a similar effect was reported by several other studies. Weitz et al. (2001) reported that nitrification decreases with increasing soil moisture contents and is predicted to cease at approximately 70% WFPS. Reduction of N_2O to N_2 is expected to start at 70% WFPS and to increase rapidly with increasing soil saturation (Weitz et al., 2001). Castaldi et al. (2013) also reported that there is a progressive reduction in the lengths dry periods in tropical forests with increases in the rainfall rates (with a peak gas flux between 30% and 35% WFPS), and these conditions are not favorable for N_2O production. Similarly, decreases in N_2O emissions in relation to the large increases in precipitation were also detected by the DyN-LPJ model (Xu et al., 2012) and Forest-DNDC model (Werner et al., 2007).

4.5. Uncertainties

Estimations of regional and global N_2O budgets have large uncertainties as a result of the high temporal and spatial variations of the input parameters within natural forests and grasslands. On one hand, COE_{NR} turns out from our model study to be a very important parameter in controlling N_2O emissions to the atmosphere. It was used to regulate the nitrification rate, therefore, the predominant sensitivity of N_2O emissions to COE_{NR} can be explained by the increase of direct N_2O production from nitrification and the availability of denitrification substrates. The experiments of MSF for COE_{NR} indicated that the variation of N_2O emissions is more likely in the range of -14.6%~+11.9%. Meteorological time series such as temperature and precipitation also have their measurement errors, thus induce some uncertainties. Most importantly, they are sensitive to the N_2O emissions. Temporal averaging and interpolation also introduce errors, for example, the LC data (0.5° × 0.5°) were resampled from 300 m resolution, which likely generated some uncertainties when calculating the global N_2O budget. Furthermore, this study tends to underestimate the N_2O fluxes, as a result of the inability to capture the peaks of N_2O emission fluxes

Table 5
Sensitivity analysis of spatial estimation.

Scenarios			Total	Tropical forests	Temperate forests	Boreal forests	Grasslands
SS		COE_{NR} value	–	0.09	0.04	0.009	0.03
		Average N_2O emissions	5.02(0.17)↑	3.03(0.15)	0.55(0.04)↑	0.04(0.005)↑	1.40(0.03)↑
SPS	P + 25%	Average N_2O emissions	5.53(0.19)↑	2.49(0.11)	1.20(0.09)↑	0.05(0.008)↑	1.79(0.04)↑
	P − 25%		4.54(0.14)↓	3.56(0.14)	0.025(0.002)↓	0.038(0.007)↓	0.92(0.02)↓
STS	T + 0.5°C	Average N_2O emissions	6.33(0.22)↑	3.13(0.13)	1.48(0.10)↑	0.05(0.009)↑	1.67(0.04)↑
	T − 0.5°C		2.35(0.40)↓	1.47(0.51)↓	0.01(0.002)↓	0.004(0.0002)↓	0.86(0.06)↓
NS		COE_{NR} value	–	0.005	0.013	0.059	0.015
		Average N_2O emissions	4.29(0.15)↑	2.63(0.13)	0.44(0.03)↑	0.03(0.004)↑	1.19(0.025)↑
MS		COE_{NR} value	–	0.014	0.044	0.124	0.044
		Average N_2O emissions	5.62(0.19)↑	3.77(0.16)	0.63(0.04)↑	0.05(0.007)↑	1.60(0.03)↑

SS: standard run with mean values of COE_{NR} for each biome region; SPS: scenario with mean values of COE_{NR} for each biome region and the variation of air temperature; STS: scenario with mean values of COE_{NR} for each biome region and the variation of precipitation; NS: the minimum scenario used a combination of minimum COE_{NR} value for every biome regions; MS: maximum scenario used a combination of maximum COE_{NR} value for every biome regions; P: daily precipitation; T: daily mean air temperature. ↓: significant decreasing trend during the period of 1992–2015; ↑: significant increasing trend during the period of 1992–2015; values in brackets denote the standard deviation (Tg N yr^{-1}).

following rewetting events, especially during the period of snowmelt in spring (Zhang et al., 2017). In addition, this study considers the effects of only atmospheric CO_2 concentrations, climate change and land cover transition on N_2O emissions and does not consider the increase in atmospheric nitrogen deposition due to human activities, which may result in the underestimation of global N_2O emissions.

5. Conclusions

The spatial and temporal patterns of N_2O fluxes from global natural forests and grasslands are estimated using the TRIPLEX-GHG model. The total N_2O emission budget was calculated by considering the variations in both fluxes and land surface areas. We found that tropical regions make large contributions to the total budgets as a result of their large N_2O flux values and large natural forest and grassland areas. The relatively large changes in N_2O emissions among years are probably due to extreme climate events. That is, N_2O emissions would increase/decrease during years with El Niño/La Niña events, which is probably related to the negative effect of precipitation on N_2O fluxes in most tropical regions. However, due to the distinct wet and dry periods in tropical grasslands, El Niño/La Niña events exert different effects on N_2O fluxes, which induced reductions/increases in N_2O during wet periods and increases/reductions in N_2O during dry periods. In addition, the results showed that soil N_2O emissions from forests are positively correlated with the atmospheric N_2O concentrations for only few months, and approximately 25.9% of total observed annual N_2O increases in the atmosphere can be explained by the total natural emissions (forests and grasslands), which implies that although there is a rising trend in N_2O emissions from natural sources (forests and grasslands in this study), other sources, including anthropogenic, riverine and oceanic N_2O sources, may be the main contributors to the elevated atmospheric N_2O concentrations at a short term. However, the absence of it in short term (interannual pattern) does not mean that the terrestrial biosphere does not affect the long-term trend in the atmosphere.

Acknowledgements

This study was financially supported by the National Key Research and Development Program of China (2016YFC0501804, 2016YFC0500203), the National Natural Science Foundation of China (41571081), the Qian-Ren Program, and a Natural Sciences and Engineering Research Council of Canada (NSERC) Discover Grant.

Appendix A. Supplementary data

Supplementary material related to this article can be found, in the online version, at doi:https://doi.org/10.1016/j.agrformet.2018.12.011.

References

Abalos, D., Brown, S.E., Vanderzaag, A.C., Gordon, R.J., Dunfield, K.E., Wagnerriddle, C., 2016. Micrometeorological measurements over 3 years reveal differences in N_2O emissions between annual and perennial crops. Glob. Change Biol. 22 (3), 1244–1255.

Artaxo, P., Berntsen, T., Betts, R., Fahey, D.W., Haywood, J., Lean, J., Lowe, D.C., Myhre, G., Nganga, J., Prinn, R., 2007. changes in atmos-pheric constituents and in radiative forcing, in climate change 2007. In: Solomon, S., Qin, D., Manning, M., Chen, Z., Marquis, M., Averyt, K.B., Tignor, M., Miller, H.L. (Eds.), The Physical Science Basis. Contribution of Working Group I to the Fourth Assessment Report of the Intergovernmental Panel on Climate Change. Cambridge University Press.

Batjes, N.H., 2006. ISRIC-WISE Derived Soil Properties on a 5 by 5 Arc-minutes Global Grid (version 1.0). ISRIC—World Soil Information, Wageningen.

Bontemps, S., Bogaert, E.V., Defourny, P., Kalogirou, V., Arino, O., 2010. GlobCover 2009 – Products Description Manual (Version 1.0). Available on the ESA IONIA website. http://ionia1.esrin.esa.int/).

Breuer, L., Papen, H., Butterbach-Bahl, K., 2000. N_2O emission from tropical forest soils of Australia. J. Geophys. Res. Atmos. 105 (D21), 26353–26367. https://doi.org/10.1029/2000JD900424.

Butterbach-Bahl, K., Stange, F., Papen, H., Grell, G., Li, C., 2000. In: van Ham, J., Baede, A.P.M., Meyer, L.A., Ybema, R. (Eds.), Impact of Changes in Temperature and Precipitation on N_2O and NO Emissions from Forest Soils, in *Non-CO_2* Greenhouse Gases: Scientific Understanding, Control and Implementation: Proceedings of the Second International Symposium. Springer Netherlands, Dordrecht, Noordwijkerhout, The Netherlands, pp. 165–171. https://doi.org/10.1007/978-94-015-9343-4_22. 8–10 September 1999.

Butterbach-Bahl, K., Baggs, E.M., Dannenmann, M., Kiese, R., Zechmeister-Boltenstern, S., 2013. Nitrous oxide emissions from soils: how well do we understand the processes and their controls? Philos. Trans. Biol. Sci. 368 (1621), 20130122.

Cai, W., Borlace, S., Lengaigne, M., Rensch, P.V., Collins, M., Vecchi, G., Timmermann, A., Santoso, A., Mcphaden, M.J., Wu, L., 2014. Increasing frequency of extreme El Nino events due to greenhouse warming. Nat. Clim. Change 4 (2), 111–116.

Castaldi, S., Bertolini, T., Valente, A., Chiti, T., Valentini, R., 2013. Nitrous oxide emissions from soil of an African rain forest in Ghana. Biogeosciences 10 (6), 4179–4187. https://doi.org/10.5194/bg-10-4179-2013.

Chatskikh, D., Olesen, J.E., Berntsen, J., Regina, K., Yamulki, S., 2005. Simulation of effects of soils, climate and management on N_2O emission from grasslands. Biogeochemistry 76 (3), 395–419. https://doi.org/10.1007/s10533-005-6996-8.

Chen, W., Zheng, X., Chen, Q., Wolf, B., Butterbach-Bahl, K., Brüggemann, N., Lin, S., 2013. Effects of increasing precipitation and nitrogen deposition on CH_4 and N_2O fluxes and ecosystem respiration in a degraded steppe in Inner Mongolia, China. Geoderma 192 (Supplement C), 335–340. https://doi.org/10.1016/j.geoderma.2012.08.018.

Ciais, P., Sabine, C., Bala, G., Bopp, L., Brovkin, V., Canadell, J., Chhabra, A., DeFries, R., Galloway, J., Heimann, M., 2014. Carbon and other biogeochemical cycles, in climate change 2013: the physical science basis. Contribution of Working Group I to the Fifth Assessment Report of the Intergovernmental Panel on Climate Change. Cambridge Univ. Press, Cambridge, U. K, pp. 465–570.

Enting, I.G., Wigley, T.M.L., Heimann, M., 1994. Future emissions and concentrations of carbon dioxide: key ocean/atmosphere/land. In: Enting, I.G., Wigley, T.M.L., Heimann, M. (Eds.), CSIRO Div. Atmos. Res. Tech. Pap. 31. CSIRO, Div. of Atmos. Res., Melbourne, Australia, pp. 133.

ESA, 2017. Land Cover CCI Product User Guide Version 2.0. [online] Available from:. http://maps.elie.ucl.ac.be/CCI/viewer/download/ESACCI-LC-Ph2-PUGv2_2.0.pdf.

Flückiger, J., Dällenbach, A., Blunier, T., Stauffer, B., Stocker, T.F., Raynaud, D., Barnola, J.-M., 1999. Variations in atmospheric N_2O concentration during abrupt climatic changes. Science 285 (5425), 227–230. https://doi.org/10.1126/science.285.5425.227.

Foley, J.A., Prentice, I.C., Ramankutty, N., Levis, S., Pollard, D., Sitch, S., Haxeltine, A., 1996. An integrated biosphere model of land surface processes, terrestrial carbon balance, and vegetation dynamics. Glob. Biogeochem. Cycles 10 (4), 603–628.

Giltrap, D.L., Li, C., Saggar, S., 2010. DNDC: a process-based model of greenhouse gas fluxes from agricultural soils. Agric. Ecosyst. Environ. 136 (3), 292–300.

Gomez-Casanovas, N., Hudiburg, T.W., Bernacchi, C.J., Parton, W.J., DeLucia, E.H., 2016. Nitrogen deposition and greenhouse gas emissions from grasslands: uncertainties and future directions. Glob. Change Biol. 22 (4), 1348–1360. https://doi.org/10.1111/gcb.13187.

Gurney, K.R., Castillo, K., Li, B., Zhang, X., 2012. A positive carbon feedback to ENSO and volcanic aerosols in the tropical terrestrial biosphere. Glob. Biogeochem. Cycles 26 (1). https://doi.org/10.1029/2011GB004129.

Hu, M., Chen, D., Dahlgren, R.A., 2016. Modeling nitrous oxide emission from rivers: a global assessment. Glob. Chang. Biol. 22 (11), 3566–3582. https://doi.org/10.1111/gcb.13351.

Huang, Y., Gerber, S., 2015. Global soil nitrous oxide emissions in a dynamic carbon-nitrogen model. Biogeosciences 12 (21), 6405–6427. https://doi.org/10.5194/bg-12-6405-2015.

Huang, B., Thorne, P.W., Banzon, V.F., Boyer, T., Chepurin, G., Lawrimore, J.H., Menne, M.J., Smith, T.M., Vose, R.S., Zhang, H., 2017. Extended reconstructed sea surface temperature, version 5 (ERSSTv5): upgrades, validations, and intercomparisons. J. Clim. 30. https://doi.org/10.1175/JCLI-D-16-0836.1.

IPCC, 2013. Climate change 2013: the physical science basis. In: Stocker, T.F., Qin, D., Plattner, G.-K., Tignor, M., Allen, S.K., Boschung, J., Nauels, A., Xia, Y., Bex, V., Midgley, P.M. (Eds.), Contribution of Working Group I to the Fifth Assessment Report of the Intergovernmental Panel on Climate Change. Cambridge University Press, Cambridge, United Kingdom and New York, NY, USA, pp. 1535. https://doi.org/10.1017/CBO9781107415324.

Kanerva, T., Palojärvi, A., Rämö, K., Manninen, S., 2008. Changes in soil microbial community structure under elevated tropospheric O_3 and CO_2. Soil Biol. Biochem. 40 (10), 2502–2510. https://doi.org/10.1016/j.soilbio.2008.06.007.

Keeling, C.D., Piper, S.C., Bacastow, R.B., Wahlen, M., Whorf, T.P., Heimann, M., Meijer, H.A., et al., 2005. Atmospheric CO_2 and $^{13}CO_2$ Exchange with the terrestrial biosphere and oceans from 1978 to 2000: observations and carbon cycle implications. In: Baldwin, I.T., Caldwell, M.M., Heldmaier, G., Jackson, R.B., Lange, O.L., Mooney, H.A., Schulze, E.D., Sommer, U., Ehleringer, J.R., Denise Dearing, M. (Eds.), A History of Atmospheric CO2 and Its Effects on Plants, Animals, and Ecosystems. Springer New York, New York, NY, pp. 83–113.

Keenan, R.J., Reams, G.A., Achard, F., de Freitas, J.V., Grainger, A., Lindquist, E., 2015. Dynamics of global forest area: results from the FAO global forest resources assessment 2015. For. Ecol. Manage. 352, 9–20. https://doi.org/10.1016/j.foreco.2015.06.014.

Kendall, M.G., 1948. Rank Correlation Methods. Griffin, Oxford, England.

Kiese, R., Hewett, B., Graham, A., Butterbach-Bahl, K., 2003. Seasonal variability of N_2O emissions and CH_4 uptake by tropical rainforest soils of Queensland, Australia. Glob. Biogeochem. Cycles 17 (2).

Kiese, R., Li, C., Hilbert, D.W., Papen, H., Butterbach-Bahl, K., 2005. Regional application of PnET-N-DNDC for estimating the N_2O source strength of tropical rainforests in the

wet tropics of Australia. Glob. Chang. Biol. 11 (1), 128–144.
Kucharik, C.J., Foley, J.A., Delire, C., Fisher, V.A., Coe, M.T., Lenters, J.D., Young-Molling, C., Ramankutty, N., Norman, J.M., Gower, S.T., 2000. Testing the performance of a dynamic global ecosystem model: Water balance, carbon balance, and vegetation structure. Glob. Biogeochem. Cycles 14 (3), 795–825. https://doi.org/10.1029/1999GB001138.
Li, C., Frolking, S., Frolking, T.A., 1992. A model of nitrous oxide evolution from soil driven by rainfall events: 1. Model structure and sensitivity. J. Geophys. Res. Atmos. 97 (D9), 9759–9776.
Li, C., Narayanan, V., Harriss, R.C., 1996. Model estimates of nitrous oxide emissions from agricultural lands in the United States. Glob. Biogeochem. Cycles 10, 297–306.
Li, C., Aber, J., Stange, F., Butterbach-Bahl, K., Papen, H., 2000. A process-oriented model of N_2O and NO emissions from forest soils: 1. Model development. J. Geophys. Res. Atmos. 105 (D4), 4369–4384.
Liu, J., Price, D.T., Chen, J.M., 2005. Nitrogen controls on ecosystem carbon sequestration: a model implementation and application to Saskatchewan, Canada. Ecol. Modell. 186 (2), 178–195.
Lu, X., Cheng, G., Xiao, F., Fan, J., 2008. Modeling effects of temperature and precipitation on carbon characteristics and GHGs emissions in Abies fabric forest of subalpine. J. Environ. Sci. 20 (3), 339–346. https://doi.org/10.1016/S1001-0742(08)60053-4.
Mann, H.B., 1945. Nonparametric tests against trend. Econometrica 13 (3), 245–259. https://doi.org/10.2307/1907187.
Matson, P.A., Vitousek, P.M., 1990. Ecosystem approach to a global nitrous oxide budget. BioScience 40 (9), 667–672. https://doi.org/10.2307/1311434.
Michaelis, L., Menten, M.L., 1913. Die Kinetik der invertinwerkung. Biochem. Z. 49 (333), 333–369.
Parton, W.J., Schimel, D.S., Cole, C.V., Ojima, D.S., 1987. Analysis of factors controlling soil organic matter levels in Great Plains Grasslands1. Soil Sci. Soc. Am. J. 51 (5), 1173–1179.
Potter, C.S., Matson, P.A., Vitousek, P.M., Davidson, E.A., 1996. Process modeling of controls on nitrogen trace gas emissions from soils worldwide. J. Geophys. Res. Atmos. 101 (D1), 1361–1377.
Raich, J.W., Potter, C.S., Bhagawati, D., 2002. Interannual variability in global soil respiration, 1980–94. Glob. Change Biol. 8 (8), 800–812. https://doi.org/10.1046/j.1365-2486.2002.00511.x.
Ravishankara, A., Daniel, J.S., Portmann, R.W., 2009. Nitrous oxide (N_2O): the dominant ozone-depleting substance emitted in the 21st century. Science 326 (5949), 123–125.
Saikawa, E., Schlosser, C.A., Prinn, R.G., 2013. Global modeling of soil nitrous oxide emissions from natural processes. Glob. Biogeochem. Cycles 27 (3), 972–989. https://doi.org/10.1002/gbc.20087.
Schwalm, C.R., Williams, C.A., Schaefer, K., Baker, I., Collatz, G.J., denbeck, C.R., 2011. Does terrestrial drought explain global CO_2 flux anomalies induced by El Niño? Biogeosciences 8 (9), 2493–2506.
Schwing, F.B., Murphree, T., deWitt, L., Green, P.M., 2002. The evolution of oceanic and atmospheric anomalies in the northeast Pacific during the El Niño and La Niña events of 1995–2001. Prog. Oceanogr. 54 (1), 459–491. https://doi.org/10.1016/S0079-6611(02)00064-2.
Shcherbak, I., Millar, N., Robertson, G.P., 2014. Global metaanalysis of the nonlinear response of soil nitrous oxide (N_2O) emissions to fertilizer nitrogen. Proc. Natl. Acad. Sci. 111 (25), 9199–9204. https://doi.org/10.1073/pnas.1322434111.
Stehfest, E., Bouwman, L., 2006. N_2O and NO emission from agricultural fields and soils under natural vegetation: summarizing available measurement data and modeling of global annual emissions. Nutr. Cycl. Agroecosyst. 74 (3), 207–228. https://doi.org/10.1007/s10705-006-9000-7.
Stocker, B.D., Roth, R., Joos, F., Spahni, R., Steinacher, M., Zaehle, S., Bouwman, L., Xu, R., Prentice, I.C., 2013. Multiple greenhouse-gas feedbacks from the land biosphere under future climate change scenarios. Nat. Clim. Chang. 3 (7), 666.
Thompson, R.L., Chevallier, F., Crotwell, A.M., Dutton, G., Langenfelds, R.L., Prinn, R.G., Weiss, R.F., Tohjima, Y., Nakazawa, T., Krummel, P.B., 2013. Nitrous oxide emissions 1999-2009 from a global atmospheric inversion. Atmos. Chem. Phys. Discuss. 13 (6), 15697–15747.
Tian, H., Chen, G., Lu, C., Xu, X., Ren, W., Zhang, B., Banger, K., Pan, S., Liu, M., Zhang, C., 2013. Global land-atmosphere exchange of methane and nitrous oxide: magnitude and spatiotemporal patterns. Biogeosci. Discuss. 10, 19811–19865. https://doi.org/10.5194/bgd-10-19811-2013.
Tian, H., Lu, C., Ciais, P., Michalak, A.M., Canadell, J.G., Saikawa, E., Huntzinger, D.N., Gurney, K.R., Sitch, S., Zhang, B., 2016. The terrestrial biosphere as a net source of greenhouse gases to the atmosphere. Nature 531 (7593), 225–228.
Tian, H., Yang, J., Lu, C., Xu, R., Canadell, J., Jackson, R., Arneth, A., Chang, J., Chen, G., Ciais, P., Gerber, S., Ito, A., Huang, Y., Joos, F., Lienert, S., Messina, P., Olin, S., Pan, S., Peng, C., Saikawa, E., Thompson, R., Vuichard, N., Winiwarter, W., Zaehle, S., Zhang, B., Zhang, K., Zhu, Q., 2018. The global N_2O model intercomparison project (NMIP): objectives, simulation protocol and expected products. Bull. Am. Meteor. Soc. 99, 1231–1251. https://doi.org/10.1175/BAMS-D-17-0212.1.
van Groenigen, K., Osenberg, C., Hungate, B., 2011. Increased soil emissions of potent greenhouse gases under increased atmospheric CO_2. Nature 475 (7355), 214–216.
Verberne, E.L.J., Hassink, J., Willigen, Pd., Groot, J.J.R., Van Veen, J.A., 1990. Modelling organic matter dynamics in different soils, Netherlands. J. Agric. Sci. 38, 221–238.
Weitz, A.M., Linder, E., Frolking, S., Crill, P.M., Keller, M., 2001. N_2O emissions from humid tropical agricultural soils: effects of soil moisture, texture and nitrogen availability. Soil Biol. Biochem. 33 (7), 1077–1093. https://doi.org/10.1016/S0038-0717(01)00013-X.
Werner, C., Butterbach-Bahl, K., Haas, E., Hickler, T., Kiese, R., 2007. A global inventory of N_2O emissions from tropical rainforest soils using a detailed biogeochemical model. Glob. Biogeochem. Cycles 21 (GB3010). https://doi.org/10.1029/2006GB002909.
Williams, E.J., Hutchinson, G.L., Fehsenfeld, F.C., 1992. NO_x and N_2O emissions from soil. Glob. Biogeochem. Cycles 6 (4), 351–388.
Xu, R., Prentice, I.C., 2008. Terrestrial nitrogen cycle simulation with a dynamic global vegetation model. Glob. Change Biol. 14 (8), 1745–1764. https://doi.org/10.1111/j.1365-2486.2008.01625.x.
Xu, X., Tian, H., Hui, D., 2008. Convergence in the relationship of CO_2 and N_2O exchanges between soil and atmosphere within terrestrial ecosystems. Glob. Change Biol. 14 (7), 1651–1660. https://doi.org/10.1111/j.1365-2486.2008.01595.x.
Xu, R., Prentice, I.C., Spahni, R., Niu, H.S., 2012. Modelling terrestrial nitrous oxide emissions and implications for climate feedback. New Phytol. 196 (2), 472–488. https://doi.org/10.1111/j.1469-8137.2012.04269.x.
Zhang, K., Peng, C., Wang, M., Zhou, X., Li, M., Wang, K., Ding, J., Zhu, Q., 2017. Process-based TRIPLEX-GHG model for simulating N_2O emissions from global forests and grasslands: model development and evaluation. J. Adv. Model. Earth Syst. 9 (5), 2079–2102. https://doi.org/10.1002/2017MS000934.
Zhu, Q., Liu, J., Peng, C., Chen, H., Fang, X., Jiang, H., Yang, G., Zhu, D., Wang, W., Zhou, X., 2014. Modelling methane emissions from natural wetlands by development and application of the TRIPLEX-GHG model. Geosci. Model. Dev. 7 (3), 981–999.
Zhu, Q., Peng, C., Chen, H., Fang, X., Liu, J., Jiang, H., Yang, Y., Yang, G., 2015. Estimating global natural wetland methane emissions using process modelling: spatio-temporal patterns and contributions to atmospheric methane fluctuations. Glob. Ecol. Biogeogr. 24 (8), 959–972. https://doi.org/10.1111/geb.12307.
Zhu, Q., Peng, C., Ciais, P., Jiang, H., Liu, J., Bousquet, P., Li, S., Chang, J., Fang, X., Zhou, X., Chen, H., Liu, S., Lin, G., Gong, P., Wang, M., Wang, H., Xiang, W., Chen, J., 2017. Interannual variation in methane emissions from tropical wetlands triggered by repeated El Niño Southern Oscillation. Glob. Change Biol. 23 (11), 4706–4716. https://doi.org/10.1111/gcb.13726.
Zhuang, Q., Lu, Y., Chen, M., 2012. An inventory of global N_2O emissions from the soils of natural terrestrial ecosystems. Atmos. Environ. 47 (Supplement C), 66–75. https://doi.org/10.1016/j.atmosenv.2011.11.036.